bioRxiv (2016) xxxxxx
doi:10.1101/xxxxxx
a Malthusian Relativity paper

$\iota^{**}=7/3\psi$
mrLife.org

The natural selection of metabolism bends body mass evolution in time

Lars Witting
Greenland Institute of Natural Resources, Box 570, DK-3900 Nuuk, Greenland

Abstract I predict a metabolic time bending of body mass evolution in the fossil record. I show that self-replication generates population dynamic feed-back selection for a body mass that increases exponentially on the per generation time-scale of natural selection, and that this increase is driven partly, or fully, by unconstrained selection for an exponential increase in mass specific metabolism. The increase in metabolism contracts natural selection time; but, mass specific metabolism evolves also by a mass-rescaling that generates a partial decline, and time dilation, with an increase in mass. The overall contraction or dilation of natural selection time is bending evolution in physical time, and this is described by an allometry $\mathrm{d}w/\mathrm{d}t \propto w^{\hat{d}t}$ for the rate of evolution in mass (w) in physical time (t).

The bending exponent ($\hat{d}t$) is shown to evolve from the relative importance of metabolism for the evolution of mass, and from the spatial dimensions of interactive competition (1D, 2D, 3D); a prediction that is shown to hold across four scale dependent bending exponents in the fossil record. The exponents are *i*) 3/2 for 2D and 5/3 for 3D evolution within a niche; as observed for horses over 57 million years of evolution. *ii*) 5/4 (2D) and 9/8 (3D) for the evolution of maximum mass across niches; as found in four mammalian clades across 30 to 64 million years of evolution. *iii*) 3/4 (2D) and 5/6 (3D) for fast body mass evolution; found for the maximum mass of trunked, and all terrestrial, mammals. And *iv*) 1 for 2D and 3D evolution along a metabolic bound, as observed across 3.5 billion years of evolution of the maximum mass in non-sessile organisms.

Keywords: Evolution, metabolism, body mass, time-bending, life history, allometry, fossil record

1 Introduction

The aggregation of inert matter in stars and planets, of organic matter in large organisms, and the associated release of energy from stars and use of energy by organisms, are some of the most striking features of our universe. An understanding of the formation and energetics of these bodies is of immense importance for science.

It is a pull from gravity that first creates stars from interstellar molecular clouds and then activates the nuclear fusion that emits energy. And energy driven self-replication in replicating molecules selects for an increased use of energy in metabolism (Witting 2016a); a use that generates net energy for self-replication and activates a population dynamic feed-back that selects for the evolution of large multicellular animals with sexual reproduction (Witting 2016b). In other words, where it is a mass driven force that forms the mass of stars and their release of energy; it is suggested that it is energy driven self-replication that selects the energy use and mass of natural organisms.

Although astronomy and evolutionary biology are rather unrelated branches of science, the scientific methods that were used to reveal this ordering of matter and energy in physics and biology were somewhat similar. Where gravity enabled Newton (1687) to explain the 3/2 exponent for the Kepler laws of planetary motion around the Sun, the population dynamic feed-back selection of energy driven self-replication enabled Witting (2016a,b) to explain the evolution of body mass allometries in biology; including a shift in the exponent for mass specific metabolism from a positive 5/6 in prokaryotes (DeLong et al. 2010) to a negative 1/4 for Kleiber (1932) scaling in multicellular animals.

This ordering of biology is predicted to spring from self-replication selection for a mass specific metabolism that generates net energy for self-replication. This is done by a net resource assimilation that is selected as a biochemical/mechanical handling of resource assimilation and the speed, or pace, of this process; with pace being selected as the mass specific work of metabolism. The unconstrained natural selection that follows generate an acceleration of biotic processes, and a steady state selection attractor where interactive competition in multicellular animals selects the increase in net energy into an exponentially increasing mass (Witting 1997, 2003).

The importance of the metabolic acceleration for this evolution of biotic mass is reflected in the body mass allometries, where the exponents are predicted to evolve as a function of the relative importance of the metabolic

pace for net resource assimilation. Witting (2016a,b) describes the natural selection of these allometric correlations across species, and I extend the theory to describe the natural selection conversion of energy into organic mass over evolutionary time, by studying body mass allometries as they unfold in time with an evolving mass. This will provide a base case for the evolution of metabolism, mass, and major life history and ecological traits in multicellular animals over time, and I test the theory by predicting body mass trajectories in the fossil record from first principles. This implies that I will use a predicted time-bend of the body mass trajectories to test for the relative importance of metabolism for the evolution of biotic masses.

1.1 Time-bend evolution

The proposed selection predicts an exponential increase in mass on the per generation time-scale of unconstrained natural selection in a stable environment (Witting 1997, 2003), given evolutionary rates that are invariant on the logarithmic scale of metabolism and mass (Witting 2016a,b). This is in agreement with fossil data where the maximum size of a clade tends to increase in a near-exponential manner during periods of phylogenetic radiation (e.g., Hayami 1978; Trammer 2005; Smith et al. 2010; Okie et al. 2013). And the correlation of evolutionary rates with the per generation time scale of natural selection is well documented both for morphological (Lynch 1990; Gingerich 1993; Okie et al. 2013) and molecular traits (Martin and Palumbi 1993; Gillooly et al. 2005; Nabholz et al. 2008; Galtier et al. 2009; Broham 2011).

The exponential increase generates a log-linear increase of mass over time, but the log-linearity is bending in physical time whenever the time-scale of natural selection is evolving with the evolutionary changes in mass (Witting 1997; Okie et al. 2013). A downward bending is induced when natural selection time is dilated by a generation time that increases with mass, and an upward bending when natural selection time is contracting from a generation time that declines with mass.

These potential bends are described by an allometry

$$\mathrm{d}w/\mathrm{d}t \propto w^{\hat{d}t} \tag{1}$$

where the rate of evolutionary change in mass ($\mathrm{d}w/\mathrm{d}t$) per unit physical time (t) is given as a power function of mass (w). The bending exponent ($\hat{d}t$) is one for unbend evolution, it is smaller than one when evolution is bending downward by a dilation of natural selection time, and it is larger than one when evolution is bending upward by a contraction of natural selection time.

From the $-1/4$ exponent of Kleiber scaling, where elephants live much longer the mice, we expect biotic time dilation and a downward bend trajectory (Okie et al. 2013). Yet the body mass trajectory of fossil horses over the past 57 million years is strongly upward bend with a $\hat{d}t$ exponent of 1.50 (Witting 1997). This indicates somewhat surprisingly that the lifespan of the horse has declined quite a bit while its mass increased from about 25 kg to 500 kg over 57 million years of evolution. I will show not only that a 3/2 exponent for the horse is likely to have emerged from a body mass selection that was driven entirely by metabolic acceleration; but more generally that mass evolution over time can be described as a continuum across four modes of selection, with each mode being supported by a unique bend of the relevant body mass trajectories in the fossil record.

1.2 Empirical test of theory

The basic idea behind my allometric model is population dynamic feed-back selection that unfolds from pre-mass selection for an exponential increase in resource handling and metabolic pace (Witting 2016a,b). The resulting increase in resource assimilation generates population growth with sustained interactive selection for an exponential increase in mass. The increase in mass is then imposing selection for a mass-rescaling, where life history traits (x) evolve allometric correlations with mass $x_w = w^{\hat{x}_w}$, where $\hat{x}_w$ is the exponent and subscript w denotes mass-rescaling. Yet, the evolution of allometries is more complex because the pre-mass selection for increased metabolism imposes a metabolic-rescaling of the life history. This rescaling is transformed into metabolic-rescaling allometries ($x_\beta = w^{\hat{x}_\beta}$) by the dependence of body mass evolution on the energy that is generated from the pre-mass acceleration of metabolic pace (subscript β denotes metabolic-rescaling). The final post-mass allometries $x = w^{\hat{x}}$ are then products $x_\beta x_w$ with exponents $\hat{x} = \hat{x}_\beta + \hat{x}_w$ that depend on the relative importance of metabolic acceleration for the evolution of the net energy of the organism.

Kleiber scaling evolves as mass-rescaling in organisms with interactive behaviour in two spatial dimensions (Witting 2016a). But as the overall scaling depends also on metabolic-rescaling, it follows that the time-bend of the log-linear trajectory in physical time is given as a function of the relative importance of metabolic acceleration. And with the time-bending exponent of eqn 1

following directly from my selection equations with no data-dependent estimates, it becomes possible to confirm, or dis-confirm, the allometric theory of population dynamic feed-back selection from time-bends in the fossil record, just as the general theory of relativity was confirmed by the bending of light around the Sun (Dyson et al. 1920).

For this test, I study four modes of selection. The first two are unconstrained natural selection within and across ecological niches. The third is fast unconstrained body mass evolution, and the last body mass evolution that proceeds along an upper bound on metabolic pace. Each of these four types of selection can be identified on theoretical grounds to trajectories that can be observed in the fossil record. The important question is then whether the observed time-bending exponents coincide with the bending exponents that follow from first principles of the selection theory.

2 Theory

For the theoretical development in this paper I assume that the reader is familiar with Witting (2016a,b), with model parameters and basic relations listed in Table 1 in Witting (2016a). I will first consider unconstrained selection with a predicted exponential increase in resource handling, metabolic pace and mass. I will then deal with the exponential evolution in relation to body mass allometries, as this will allow me to deduce life history evolution on the per generation time-scale. And when the per generation allometry for the evolution of generation time with mass is combined with the per generation increase in mass, I can predict body mass evolution in physical time; as observed in the fossil record.

2.1 Unconstrained selection

My earlier studies have found that large body masses are selected by a population dynamic feed-back selection, where the energy that is allocated into reproduction generates population growth that generates interactive competition that selects the energy into mass at the cost of replication and a continued increase in the density of the population (Witting 1997, 2003, 2016b). This population dynamic selection pressure on mass, and the selected mass, are primarily dependent upon the net energy of the average individual (ϵ) in the population, as it is this energy that generates the population growth and interactive selection in the population.

This net assimilated energy

$$\epsilon = \alpha\dot{\beta} \tag{2}$$

is a product between the handling of resource assimilation [$\alpha = \ddot{\alpha}\rho^{**}$, given by intrinsic handling ($\ddot{\alpha}$) at the equilibrium resource density ρ^{**}], and the pace ($\dot{\beta} = \beta/\dot{W}$) of this process, with pace being selected as a proxy of mass specific metabolism (β, Witting 2016a).

As the per generation replication rate ($\lambda = p\,t_r\epsilon/\tilde{\beta}w = 1$) is proportional with ϵ, the per generation selection gradients on the three resource assimilation parameters $x \in \{\epsilon, \alpha, \dot{\beta}\}$ are unity on logarithmic scale

$$\partial r/\partial \ln x = 1 \tag{3}$$

Then, from the secondary theorem of natural selection ($\mathrm{d}x/\mathrm{d}\tau = \sigma_x^2 \partial r/\partial x$, Robertson 1968; Taylor 1996) and invariant heritable variation on log-scale ($\sigma^2_{\ln x}$) we expect an exponential increase

$$\begin{aligned} r_\epsilon &= \mathrm{d}\ln\epsilon/\mathrm{d}\tau = \sigma^2_{\ln\epsilon} \\ r_\alpha &= \mathrm{d}\ln\alpha/\mathrm{d}\tau = \sigma^2_{\ln\alpha} \\ r_{\beta_\beta} &= \mathrm{d}\ln\beta_\beta/\mathrm{d}\tau = \sigma^2_{\ln\beta} \end{aligned} \tag{4}$$

where the increase in net energy

$$r_\epsilon = r_\alpha + r_{\beta_\beta} \tag{5}$$

is given by the increase in the two subcomponents.

This metabolic increase relates to the pre-mass component β_β that distinguishes this primary increase from the decline (β_w) of the secondary mass-rescaling that evolves from an increase in mass. This distinction is not relevant for resource handling (α), as it is a pure pre-mass parameter that is generating net energy for the selection of mass. The distinction between a pre-mass and a rescaling component is also not relevant for the primary increase in net energy, because the net energy on the per generation time-scale of natural selection is invariant of mass-rescaling (Witting 2016a).

The increase in net resource assimilation generates population growth with a density dependent equilibrium, where the level of interactive competition

$$\iota^* = (\gamma_\iota/\gamma)\ln(\tilde{\epsilon}_0/w) \tag{6}$$

is as a function of net energy $\tilde{\epsilon}_0 = pt_r\epsilon_u\bar{f}\left(vh^{\frac{d-1}{d}}\right)^\gamma/\tilde{\beta}$, with ϵ_u being net energy on the unexploited resource (Witting 2016a). The result is population dynamic feed-back selection where the resulting rate of increase in mass

$$r_w = \mathrm{d}\ln w/\mathrm{d}\tau = \sigma^2_{\ln w}[(\psi\gamma_\iota/\gamma)\ln(\tilde{\epsilon}_0/w) - 1] \tag{7}$$

is a product between the selection gradient $[\partial r_i^*/\partial \ln w_i|_{w_i=w} = (\psi\gamma_\iota/\gamma)\ln(\tilde{\epsilon}_0/w) - 1]$ that includes the population dynamic pressure of interactive

competition (Witting 2016b) and the heritable variance ($\sigma^2_{\ln w}$).

As the $\tilde{\epsilon}_0/w$ component of eqn 7 is invariant of mass (Witting 2016a), the expected increase is exponential, and it may thus be rewritten as

$$\frac{\mathrm{d}\ln w}{\mathrm{d}\tau} = \frac{\partial \ln w}{\partial \ln \epsilon}\frac{\mathrm{d}\ln \epsilon}{\mathrm{d}\tau} \tag{8}$$

with an invariant selection relation

$$\partial \ln w/\partial \ln \epsilon = 1/\hat{\epsilon} \tag{9}$$

Hence, we have

$$r_w = r_\epsilon/\hat{\epsilon} \tag{10}$$

and a natural selection that defines mass

$$w = \int \frac{\partial \ln w}{\partial \ln \epsilon}\,\mathrm{d}\ln \epsilon = (\epsilon/\bar{\epsilon}_\circ)^{1/\hat{\epsilon}} \tag{11}$$

by the inverse of the energetic allometry

$$\epsilon = \bar{\epsilon}_\circ w^{\hat{\epsilon}} \tag{12}$$

where $\hat{\epsilon} = (2d-1)/2d$ is the predicted exponent from Witting (2016a), $\bar{\epsilon}_\circ$ the intercept, and d the spatial dimensionality of intra-specific interactions.

By setting eqn 10 equal to eqn 7 we find the mass of the steady state

$$\begin{aligned} w^{**}_\tau &= \tilde{\epsilon}_{0,\tau} e^{-(1+r_\epsilon/\sigma^2_{\ln w}\hat{\epsilon})\gamma/\gamma_\iota\psi} \\ &= p\, t_r \epsilon_\tau/\tilde{\beta}, \end{aligned} \tag{13}$$

with

$$\begin{aligned} r_w &< r_\epsilon/\hat{\epsilon} \quad \text{for} \quad w > w^{**} \\ r_w &> r_\epsilon/\hat{\epsilon} \quad \text{for} \quad w < w^{**} \end{aligned} \tag{14}$$

that confirms that the steady state is the unconstrained selection attractor for mass.

If we then insert eqn 6 into eqn 7, and set $r_w = r_\epsilon/\hat{\epsilon}$ from eqn 10, we find that the level of intra-specific interference competition

$$\iota^{**} = (1 + r_\epsilon/\sigma^2_{\ln w}\hat{\epsilon})/\psi \tag{15}$$

for an exponentially evolving mass is somewhat higher than that of a stable mass at an equilibrium attractor with an upper constraint on net energy (Witting 2016b). As the parameters on the right hand side of eqn 15 are expected to be body mass invariant, we note that the theoretically deduced allometries (Witting 1995, 2016a) apply also for body mass evolution at steady state. As already noted, this implies an energetic exponent of $\hat{\epsilon} = (2d-1)/2d$, and with $r_\epsilon = \sigma^2_{\ln \epsilon}$ from eqn 4, we find that the level of interference reduces to

$$\iota^{**} = \frac{4d-1}{2d-1}\frac{1}{\psi} \tag{16}$$

for the symmetrical case where $\sigma^2_{\ln w} = \sigma^2_{\ln \epsilon}$. The position of this selection attractor of the steady state is shown on the selection integral in Fig. 1f in Witting (2016b).

Nearly all the allometries considered here and in Witting (2016a) are inter-specific allometries that describe the variation in the average trait of evolved populations; either across species (Witting 2016a) or along evolutionary lineages in time (current paper). Yet, the evolutionary steady state defines also an important intra-specific allometry that describes the correlation between reproduction and mass across the individuals in the evolving population. To obtain this allometry, insert eqn 16 into the selection gradient $\partial r^*_i/\partial \ln w_i|_{w_i=w} = \psi\iota^* - 1$ for the multicellular animal in Witting (2016b) and integrate over $\ln w_i$ to find that the within population variation in the pR-product scale as

$$p_i R_i \propto w_i^{2d/(2d-1)} \tag{17}$$

As this exponent is 4/3 and 6/5 for organisms with intra-specific interactions in two and three spatial dimensions, we find a reproductive rate that is about proportional to mass when survival is relatively invariant. This proportionality is observed in natural populations (Peters 1983) and it reflects a level of interactive competition that is so high that resource monopolization scales to the approximate second power of mass.

2.2 Allometries in time

The predicted exponential increase in metabolism and mass on the per generation time-scale of unconstrained natural selection is an essential finding for evolutionary biology in itself. But to understand its implication in detail, we need to transform the prediction into physical time so that it can be compared with data from the fossil record. For this we need to predict the correlated evolution between mass and the per generation time-scale of natural selection.

This correlation is given by the allometries in this subsection; with allometries predicted not only for the generation time that is needed for the time-transformation of the body mass trajectory, but also for a larger set of traits that allow for more general predictions of life history evolution in time. For this deduction we have most of the theory in place. We have an evolutionary steady state with an exponential increase in resource handling (α), pace ($\dot{\beta} \propto \beta$), net

energy (ϵ) and mass (w), and a set of post-mass allometries that describes how the generation time is evolving with mass (Witting 2016a). We need, however, to deal in more detail with the transformation of evolution in time because this will depend, as we will see, on the underlying causes for the evolution of mass.

Recall that the exponents of the final post-mass allometries evolve as a combination of exponents that evolve from the metabolic-rescaling of the life history and exponents that evolve from mass-rescaling. The latter reflects the selection response of the life history to the selection pressure on mass, and they are independent of the underlying causes for the evolutionary variation in net energy (Witting 2016a). The metabolic-rescaling exponents that emerge from the scaling of the life history from the pre-mass selection of metabolic pace, however, depend on the underlying causes (α versus β) for the variation in net energy.

The evolution of these two types of exponents relate to the evolution of traditional Kleiber allometries, where the exponent for mass specific metabolism in $-1/2d$. The mass-rescaling exponents are the exponents of these Kleiber allometries, with the metabolic-rescaling exponents representing the scaling of the intercepts of these allometries, as they evolve from primary selection on metabolic pace.

In order to deduce the time evolution of these intercepts, we have from eqns 5 and 10 that

$$r_w = r_\epsilon/\hat{\epsilon} = (r_\alpha + r_{\beta_\beta})/\hat{\epsilon} \tag{18}$$

Now let

$$\begin{aligned} \hat{\alpha} &= r_\alpha/r_w &= r_\alpha\,\hat{\epsilon}/(r_\alpha + r_{\beta_\beta}) \\ \hat{\beta}_\beta &= r_{\beta_\beta}/r_w &= r_{\beta_\beta}\hat{\epsilon}/(r_\alpha + r_{\beta_\beta}) \end{aligned} \tag{19}$$

The exponential increase in α, β_β, ϵ and w on the per generation time-scale may then be expressed as

$$\begin{aligned} \alpha_\tau &= \alpha_0 e^{\hat{\alpha} r_w \tau} \\ \beta_{\beta,\tau} &= \beta_{\beta,0} e^{\hat{\beta}_\beta r_w \tau} \\ \epsilon_\tau &= \epsilon_0 e^{\hat{\epsilon} r_w \tau} \\ w_\tau &= w_0 e^{r_w \tau} \end{aligned} \tag{20}$$

From these equations we can construct time allometries. For this, solve the body mass relation for time $\tau = \ln(w_\tau/w_0)/r_w$. Insert this time into the other relations and obtain

$$\begin{aligned} \alpha_\tau &= \bar{\alpha}_\circ w_\tau^{\hat{\alpha}} \\ \beta_{\beta,\tau} &= \bar{\beta}_\circ w_\tau^{\hat{\beta}_\beta} \\ \epsilon_\tau &= \bar{\epsilon}_\circ w_\tau^{\hat{\epsilon}} \end{aligned} \tag{21}$$

with intercepts $\bar{\alpha}_\circ = \alpha_0/w_0$, $\bar{\beta}_\circ = \beta_{\beta,0}/w_0$, and $\bar{\epsilon}_\circ = \epsilon_0/w_0$. Hence, from eqn 19 and $\hat{\epsilon} = (2d-1)/2d$, we find that these time allometries

$$\begin{aligned} \beta_{\beta,\tau} &= \bar{\beta}_\circ w_\tau^{\frac{1}{1+r_\alpha/r_{\beta_\beta}}\frac{2d-1}{2d}} \\ \alpha_\tau &= \bar{\alpha}_\circ w_\tau^{\frac{1}{1+r_{\beta_\beta}/r_\alpha}\frac{2d-1}{2d}} \\ \epsilon_\tau &= \bar{\epsilon}_\circ w_\tau^{\frac{2d-1}{2d}} \end{aligned} \tag{22}$$

depend on the spatial dimensionality of the interactive behaviour (d), and on the r_{β_β}/r_α-ratio of the rates of increase in pace over handling.

The dependence of the allometric exponent for mass specific metabolism on the r_{β_β}/r_α-ratio is illustrated in Fig. 1. A constant mass-rescaling intercept with $\hat{\beta}_\beta = 0$ is obtained only when $r_{\beta_\beta}/r_\alpha = 0$. More generally the intercept will increase with an evolutionary increasing body mass, because the mass increase is driven partly, or fully, by the evolutionary increase in mass specific metabolism. For symmetrical unconstrained evolution where $r_{\beta_\beta}/r_\alpha = 1$, the mass-rescaling intercept will increase to the 3/8 power of body mass in 2D, and the 5/12 power in 3D. And at the limit where metabolism is evolving unconstrained ($r_{\beta_\beta} > 0$) while resource handling is constrained ($r_\alpha = 0$) and $r_{\beta_\beta}/r_\alpha \approx \infty$, we find the mass-rescaling intercept for mass specific metabolism to scale to the 3/4 power in 2D, and the 5/6 power in 3D.

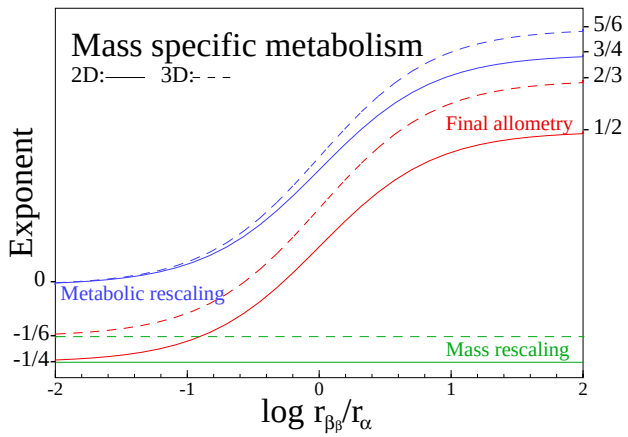

Figure 1: **The allometric scaling** of mass specific metabolism ($\beta \propto w^{\hat{\beta}} \propto w^{\hat{\beta}_\beta} w^{\hat{\beta}_w}$) as it evolves from the r_{β_β}/r_α-ratio given 2D and 3D interactions. The blue curves are the exponents of metabolic-rescaling ($\hat{\beta}_\beta$), the green lines the exponents of mass-rescaling ($\hat{\beta}_w$), and the red curves the exponents of the final post-mass allometries ($\hat{\beta} = \hat{\beta}_\beta + \hat{\beta}_w$).

From the inverse relation $\tau \propto 1/\dot{\beta}$ between biotic time and metabolic pace, we find biotic time to evolve with metabolic-rescaling as

$$\tau_{\beta,\tau} = \bar{\tau}_{\circ} w_{\tau}^{\frac{1}{1+r_{\alpha}/r_{\beta_{\beta}}}\frac{1-2d}{2d}} \tag{23}$$

and mass-rescaling as

$$\tau_{w,\tau} = w_{\tau}^{1/2d} \tag{24}$$

Where mass-rescaling dilates natural selection time with a decline in metabolic pace as the mass increases by natural selection, we find quite generally that the mass-rescaling intercept of biotic time will decline with an evolutionary increasing mass, a process that causes a contraction of natural selection time. Whether natural selection time will actually contract or dilate will depend upon the scaling of metabolic-rescaling relative to mass-rescaling with the final post-mass allometry for biotic time evolving as

$$\tau_{\tau} = \bar{\tau}_{\circ} w_{\tau}^{\left(\frac{1}{1+r_{\beta_{\beta}}/r_{\alpha}} - \frac{2(d-1)}{1+r_{\alpha}/r_{\beta_{\beta}}}\right)/2d} \tag{25}$$

This implies that natural selection time will dilate to the 1/4 power in 2D and the 1/6 power in 3D only when there is no evolutionary increase in the mass-rescaling intercept for mass specific metabolism. It will remain constant and body mass invariant when $r_{\beta_{\beta}}/r_{\alpha} = 1/2(d-1)$, i.e., 1/2 in 2D and 1/4 in 3D, and contract to the $-1/8$ power in 2D and the $-1/4$ power in 3D for symmetrical unconstrained evolution ($r_{\beta_{\beta}}/r_{\alpha} = 1$). At the $r_{\beta_{\beta}}/r_{\alpha} \approx \infty$ limit where body mass is increasing exclusively because of an increasing metabolic rate, the contraction of natural selection time will occur to the $-1/2$ power in 2D and the $-2/3$ power in 3D.

A more complete set of post-mass exponents for exponentially evolving masses is shown in Table 1, and they are obtained from eqn 22 in combination with the metabolic-rescaling exponents and mass-rescaling exponents from Table 1 in Witting (2016a).

a) One dimensional interactions ($\hat{\epsilon} = 1/2$)

$\frac{r_{\beta_{\beta}}}{r_{\alpha}}$	$\hat{\alpha}$	$\hat{\beta}$	$\hat{\tau}$	$\hat{p}$	$\hat{R}$	$\hat{r}$	$\hat{h}$	$\hat{n}$	$\hat{dt}$
0	$\frac{1}{2}$	$-\frac{1}{2}$	$\frac{1}{2}$	0	0	$-\frac{1}{2}$	1	$-\frac{1}{2}$	$\frac{1}{2}$
1	$\frac{1}{4}$	$-\frac{1}{4}$	$\frac{1}{4}$	$\frac{1}{4}$	$-\frac{1}{4}$	$-\frac{1}{4}$	1	$-\frac{3}{4}$	$\frac{3}{4}$
∞	0	0	0	$\frac{1}{2}$	$-\frac{1}{2}$	0	1	-1	1

b) Two dimensional interactions ($\hat{\epsilon} = 3/4$)

$\frac{r_{\beta_{\beta}}}{r_{\alpha}}$	$\hat{\alpha}$	$\hat{\beta}$	$\hat{\tau}$	$\hat{p}$	$\hat{R}$	$\hat{r}$	$\hat{h}$	$\hat{n}$	$\hat{dt}$
0	$\frac{3}{4}$	$-\frac{1}{4}$	$\frac{1}{4}$	0	0	$-\frac{1}{4}$	1	$-\frac{3}{4}$	$\frac{3}{4}$
$\frac{1}{2}$	$\frac{1}{2}$	0	0	$\frac{1}{4}$	$-\frac{1}{4}$	0	1	-1	1
1	$\frac{3}{8}$	$\frac{1}{8}$	$-\frac{1}{8}$	$\frac{3}{8}$	$-\frac{3}{8}$	$\frac{1}{8}$	1	$-\frac{9}{8}$	$\frac{9}{8}$
∞	0	$\frac{1}{2}$	$-\frac{1}{2}$	$\frac{3}{4}$	$-\frac{3}{4}$	$\frac{1}{2}$	1	$-\frac{3}{2}$	$\frac{3}{2}$

c) Three dimensional interactions ($\hat{\epsilon} = 5/6$)

$\frac{r_{\beta_{\beta}}}{r_{\alpha}}$	$\hat{\alpha}$	$\hat{\beta}$	$\hat{\tau}$	$\hat{p}$	$\hat{R}$	$\hat{r}$	$\hat{h}$	$\hat{n}$	$\hat{dt}$
0	$\frac{5}{6}$	$-\frac{1}{6}$	$\frac{1}{6}$	0	0	$-\frac{1}{6}$	1	$-\frac{5}{6}$	$\frac{5}{6}$
$\frac{1}{4}$	$\frac{2}{3}$	0	0	$\frac{1}{6}$	$-\frac{1}{6}$	0	1	-1	1
1	$\frac{5}{12}$	$\frac{1}{4}$	$-\frac{1}{4}$	$\frac{5}{12}$	$-\frac{5}{12}$	$\frac{1}{4}$	1	$-\frac{5}{4}$	$\frac{5}{4}$
∞	0	$\frac{2}{3}$	$-\frac{2}{3}$	$\frac{5}{6}$	$-\frac{5}{6}$	$\frac{2}{3}$	1	$-\frac{5}{3}$	$\frac{5}{3}$

Table 1: **Theoretical allometries.** Allometric exponents ($\hat{x}$) for exponential body mass evolution in time, as they evolve from allometric rescaling with selection on mass and metabolic pace. The exponents depend on the dimensionality of the interactive behaviour, and on the ratio of the exponential rate of increase in metabolic pace over resource handling ($r_{\beta_{\beta}}/r_{\alpha}$). **Symbols**: ϵ:net energy; α:resource handling; β:mass specific metabolism; τ:biotic periods/time; p:survival; R:lifetime reproduction; r:population growth rate; h:home range; n:population density; $\hat{dt}$:rate of body mass evolution.

2.3 Mass in physical time

With the equations for the evolution of handling, pace and mass on a per generation time-scale (eqns 20 and 22), and the associated allometric scaling with mass (Table 1), we have a predictive theory for unconstrained life history evolution in time. The evolution of the exponential mass trajectory will depend primarily on the per generation rate of change in mass (r_w from eqns 7 and 18), with the remaining life history being a function of the evolving mass (Table 1); with the functional relationship being dependent both upon the underlying causes for the exponential increase in net energy (the $r_{\beta_{\beta}}/r_{\alpha}$-ratio) and the number of spatial dimensions of the competitive behaviour between the individuals in the evolving population.

With this evolution being expressed on the per generation time-scale of natural selection it is not directly comparable with evolutionary trajectories from the fossil record. The majority of the involved life history traits are furthermore impossible to estimate from fossil data, implying that no direct verification is possible. The exception is body mass; the life history trait that often is estimated from fossil data.

To transform the predicted body mass trajectories to the physical time-scale of the fossil record, we have that

the rate of change in mass in physical time is

$$\mathrm{d}w/\mathrm{d}t = (\mathrm{d}w/\mathrm{d}\tau)/\tau = r_w w/\tau \tag{26}$$

Then, from eqn 25 we obtain the following allometry

$$\mathrm{d}w/\mathrm{d}t = \tilde{r_w} w^{\hat{d}t}, \tag{27}$$

for the rate of evolutionary change in mass, where

$$\hat{d}t = \left(\frac{2}{1 + r_\alpha/r_{\beta_\beta}} + \frac{1}{1 + r_{\beta_\beta}/r_\alpha}\right)\frac{2d-1}{2d}, \tag{28}$$

and $\tilde{r_w} = r_w/\bar{\tau}_\circ$. The $\hat{d}t$ exponent is presented in Table 1 as a function of the r_{β_β}/r_α-ratio given intraspecific interactions in one, two, and three spatial dimensions.

All of the predicted mass trajectories of unconstrained selection are log-linear on the per generation time-scale of natural selection. The corresponding trajectories in physical time may bend downward ($\hat{d}t < 1$) or upward ($\hat{d}t > 1$) to some degree depending upon the r_{β_β}/r_α-ratio and the spatial dimensionality of the interactive behaviour. This time-bending is illustrated in Fig. 2, with the evolutionary trajectory being log-linear in physical time ($\hat{d}t = 1$) only when the r_{β_β}/r_α-ratio is $1/2(d-1)$ (yellow trajectory).

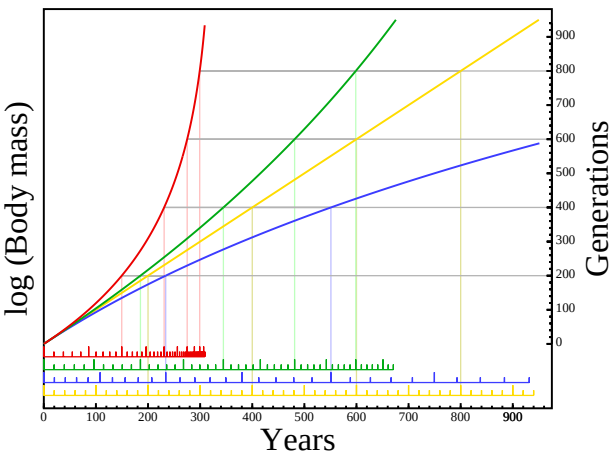

Figure 2: **Evolutionary bending** by contraction and dilation of natural selection time. A theoretical illustration of body mass (w) evolution when the rate of exponential increase [$r_w = (r_\alpha + r_{\beta_\beta})/\hat{\epsilon}$] is constant on the per generation time-scale of natural selection (2D interactions). The initial generation time is a year for all lineages, and the per generation time-scale (right y-axis) is shown in physical time by the coloured x-axis. The degree of bending follows from the r_{β_β}/r_α-ratio, and there is only a downward bend from time dilation when $r_{\beta_\beta}/r_\alpha = 0$ (**blue**). Time dilation and contraction are equally strong (with no overall bending) when $r_{\beta_\beta}/r_\alpha = 1/2(d-1)$ (**yellow**), while contraction with upward bending is dominating for unconstrained symmetrical evolution ($r_{\beta_\beta}/r_\alpha = 1$, **green**) and extreme for within niche evolution with resource handling at an evolutionary optimum ($r_{\beta_\beta}/r_\alpha \approx \infty$, **red**).

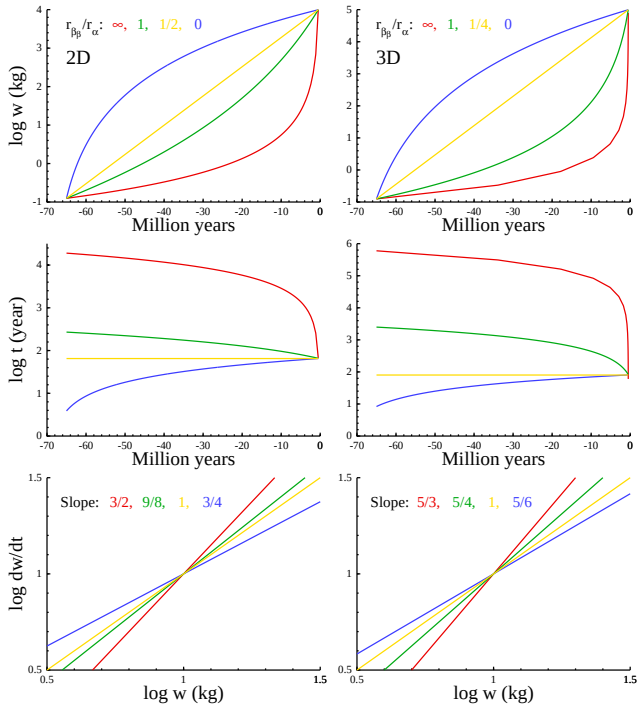

Figure 3: **Theoretical curves** for the evolution of maximum mammalian mass (w; **top**), with lifespan (t; **middle**), in physical time, given constant rates of evolution for 2D and 3D interactions. The r_{β_β}/r_α-ratio can be estimated by the slope (eqn 28) of the allometry for evolutionary increase in body mass (dw/dt, kg per million year) in physical time (**bottom**).

In order to illustrate these findings more directly to evolution on Earth, given constant rates of evolution for different r_{β_β}/r_α-ratios, Fig. 3 shows the span of possible evolutionary trajectories in lifespan and body mass from an estimated 125 gram ancestor for placental mammals that lived 65 million years ago (MA; O'Leary et al. 2013) to a 10 tonnes terrestrial (2D) and 100 a tonnes pelagic (3D) mammal today. Included are also the $\hat{d}t$ exponents of the associated allometries for the evolutionary increase in mass (eqn 28).

The shapes of the trajectories are dependent upon the r_{β_β}/r_α-ratio. When zero, the net energy and body mass are increasing exclusively because of improved resource handling, and there is no evolutionary change in mass specific metabolism except for the decline im-

posed by the rescaling of the life history in response to the evolutionary increase in mass. The log trajectory is then levelling off over time with a downward bend and a $\mathrm{d}w/\mathrm{d}t$ exponent of 3/4 or 5/6, dependent upon dimensionality. At the other extreme, the r_{β_β}/r_α-ratio is infinite, the energetic increase is exclusively due to enhanced metabolism, and the log trajectory is bend strongly upward with a $\mathrm{d}w/\mathrm{d}t$ exponent of 3/2 or 5/3. In between, the trajectory will have a smaller upward bend when the ratio is one, and it is linear when the ratio is 1/2 in 2D and 1/4 in 3D.

Some of these theoretical findings may appear intuitively more plausible than others. Being familiar with Kleiber scaling, where elephants live much longer than mice, a downward bend trajectory with a 3/4 $\mathrm{d}w/\mathrm{d}t$ exponent is in agreement with common conception. A strongly upward bend trajectory with a $\mathrm{d}w/\mathrm{d}t$ exponent of 5/3 and a lifespan that declines to the negative 2/3 power of mass, however, is clearly beyond common knowledge obtained from studies of existing species on Earth. Hence, in order to enhance our understanding of the different modes of natural selection on mass, I describe in the next four subsections the ecological and physiological conditions behind each of the four selection modes in Figs. 2 and 3.

2.3.1 *Evolution within niches* ($r_{\beta_\beta}/r_\alpha \approx \infty$)

A r_{β_β}/r_α-ratio that approaches infinity can be expected for evolutionary lineages that evolve by unconstrained selection within a stable ecological niche. The handling of the resource is then optimised by natural selection, and when handling is at a selection optimum it follows that $r_\alpha \to 0$. The net energy, and thus also mass, can then only increase by natural selection for increased metabolic pace, implying that $r_{\beta_\beta}/r_\alpha \to \infty$. These lineages will have a $\mathrm{d}w/\mathrm{d}t$ exponent of $(2d-1)/d$, with body mass trajectories that are bend strongly upward in physical time due to a time contraction where the time-scale of natural selection evolves as $\tau_\tau \propto w_\tau^{(1-d)/d}$.

This evolution is dependent upon a mass specific metabolism that can evolve unconstrained below a potential upper limit. Such evolution may be initiated from an upper metabolic limit, when preceded by evolution where $r_{\beta_\beta}/r_\alpha < 1/2(d-1)$ and mass specific metabolism is declining with an evolutionary increase in mass.

2.3.2 *Evolution across niches* ($r_{\beta_\beta}/r_\alpha = 1$)

A r_{β_β}/r_α-ratio around unity can be expected for unconstrained symmetrical selection, that may occur when resource handling is free to evolve across ecological niches and there are no evolutionary constrains on mass specific metabolism and mass. While these conditions may rarely apply over longer time-scales for evolution within ecologically adapted species (where $r_\alpha \to 0$ as $t \to \infty$), the conditions may easily exists for the largest species of a taxonomic group when the group diversifies into a plenitude of species through adaptation to a multitude of ecological niches. During such evolutionary radiation it is only the larger species, which are dominant in inter-specific interactions, that can be expected to have unconstrained selection on resource handling across niches, as niche access for the smaller species is likely to be restricted by inter-specific interactions with larger species.

Evolution with a r_{β_β}/r_α-ratio around one may thus be our base case expectation for the evolution of maximum mass within taxonomic groups over time. These trajectories will have a $\mathrm{d}w/\mathrm{d}t$ exponent of $(6d-3)/4d$, and for both 2D and 3D evolution they will have a slight upward bend in physical time due to a time contraction where natural selection time evolves as $\tau_\tau \propto w_\tau^{(3-2d)/4d}$.

2.3.3 *Fast body mass evolution* ($r_{\beta_\beta}/r_\alpha = 0$)

A r_{β_β}/r_α-ratio of about zero is expected when evolution in resource handling is outrunning evolution in metabolic pace. A first though might suggest that this will occur as a consequence of a mass specific metabolism that is upward constrained. This is, however, not the case because the mass-rescaling from the evolutionary increase in mass that follows from an increase in α will cause mass specific metabolism to decline below the upper bound. Selection on mass specific metabolism is then no longer constrained.

A r_{β_β}/r_α-ratio around zero requires instead that resource handling evolves much faster than metabolic pace. This may occur when resource handling evolves across niches and the density of the resource is increasing across this gradient. The net energy that is assimilated during a resource handling cycle is then increasing faster than the natural selection induced evolution in the handling efficiency of the cycle. A r_{β_β}/r_α-ratio around zero may also occur if the resource handling efficiency is increasing as a mechanistic function of the evolutionary increase in mass.

Irrespectively of the underlying mechanistic cause, we can expect r_{β_β}/r_α-ratios around zero to be associated with fast body mass evolution, as α is required to increase much faster than the back-ground selected increase in mass specific metabolism. Hence, this type of evolution may be expected for the evolution of the

largest species during an evolutionary radiation. Such exponential evolution will have a $\mathrm{d}w/\mathrm{d}t$ exponent of $(2d-1)/2d$, and a downward bend curve in physical time due to a time dilation where the time-scale of natural selection is evolving as $\tau_\tau \propto w_\tau^{1/2d}$.

2.3.4 *Evolution at metabolic limit* $\left(\frac{r_{\beta_\beta}}{r_\alpha} = \frac{1}{2d-2}\right)$

A forth type of mass evolution will occur when mass specific metabolism is evolving along an upper bound; a selection that coincides with a r_{β_β}/r_α exponent of $1/2(d-1)$. An initial increase in mass will then require an initial increase in resource handling, as the metabolic pace cannot increase beyond the upper bound. The mass-rescaling from the associated increase in mass will generate a decline in mass specific metabolism as it evolves along an allometric scaling with a negative $1/2d$ exponent. This will free mass specific metabolism from its upper bound, allowing for a selection increase back to the bound, unless the evolution in resource handling occurs too fast. The result is a constant mass specific metabolism over time ($\hat{\beta} = 0$), which implies $\hat{\beta}_\beta = -\hat{\beta}_w = 1/2d$ and $r_{\beta_\beta}/r_\alpha = 1/2(d-1)$.

This evolution may be expected across time-scales that are much larger than the time-scales of evolutionary radiation of taxonomic groups. At these scales, we may expect species to be well adapted to their niches, with relatively little evolution in resource handling. And we may also expect natural selection on metabolic pace to have occurred so long that it has taken mass specific metabolism to an upper bound.

3 Evidence

3.1 Fossil mammals

3.1.1 *Fossil horses*

A r_{β_β}/r_α-ratio about infinity is expected when evolution in resource handling is negligible compared with evolution in metabolic pace. Time contraction (eqn 23) is then bending the evolutionary trajectory to the 3/4 power of mass in 2D and 5/6 power in 3D, with $\mathrm{d}w/\mathrm{d}t$ exponents around 3/2 for 2D, and 5/3 for 3D.

This is predicted for lineages that evolve within an ecological niche, with within lineage data from horse (Equidae) fossils (MacFadden 1986) over 57 million years of evolution being spot on with a 2D dw/dt exponent of 1.50 ± 0.17 (Fig. 4).

We may thus conclude that horses evolved large masses almost exclusively through process acceleration with strong time contraction. This implies that a 25 kg horse that lived 57 MA had a lifespan around 90 years, given a 20 year lifespan of a 500 kg horse today. If there had been no selection on process speed, we should still have 25 kg horses with 90 year lifespans, and if horses had increased in size due to resource handling alone we should have 500 kg horses that live for 200 years.

This mass evolution was dependent on a mass specific metabolism that was relatively far from its upper bound in horses 57 million years ago. And the early horse might be an excellent example of a species with a mass specific metabolism that was reset by early mammalian evolution. Assuming a stable evolution of process speed, we calculate that an increase from a 125 gram ancestor at 65 MA (O'Leary et al. 2013) to a 25 kg horse at 57 MA would require a r_{β_β}/r_α-ratio around 1/15. The associated proportional decline in mass specific metabolism is calculated to about 0.27, which is approximately the inverse of the 4.7 times increase in mass specific metabolism that evolved from 57 to 0 MA when horses increased to 500 kg due to metabolic acceleration. Hence, even with a mass specific metabolism that increased exponentially in horses over 57 million years of evolution, the mass corrected metabolism is estimated to be about the same in todays horses and the mammalian ancestor that lived 65 million years ago.

3.1.2 *Maximum mass of mammalian clades*

If we increase the ecological scale we have a r_{β_β}/r_α-ratio around one that represents unconstrained symmetrical evolution in process speed, resource handling and mass; to be expected when resource handling is free to evolve across ecological niches. The bending powers of process acceleration (eqn 23) are then 3/8 in 2D and 5/12 in 3D, with associated $\mathrm{d}w/\mathrm{d}t$ exponents of 9/8 and 5/4.

This evolution is approximated by the maximum body mass in four out of five mammalian clades (Fig. 4, table). As expected, 2D $\mathrm{d}w/\mathrm{d}t$ exponents around 1.13 are observed over 64 million years of evolution in terrestrial carnivores (Carnivora/Fissipedia) and 50 million years in even-toed ungulates (Artiodactyla). Alternative 3D exponents around 1.23 are observed across 30 million years of evolution in whales (Cetacea & Mysticeti) and 55 million years in primates (Primates). As pelagic and tree living species, the individuals of these taxa have an extra vertical dimension in their interactive behaviour.

Relating to the example of whales, we estimate a lifespan around 275 years for a 410 kg ancestor that lived 31 MA, given a 70 year lifespan of a 100 tonne blue whale today.

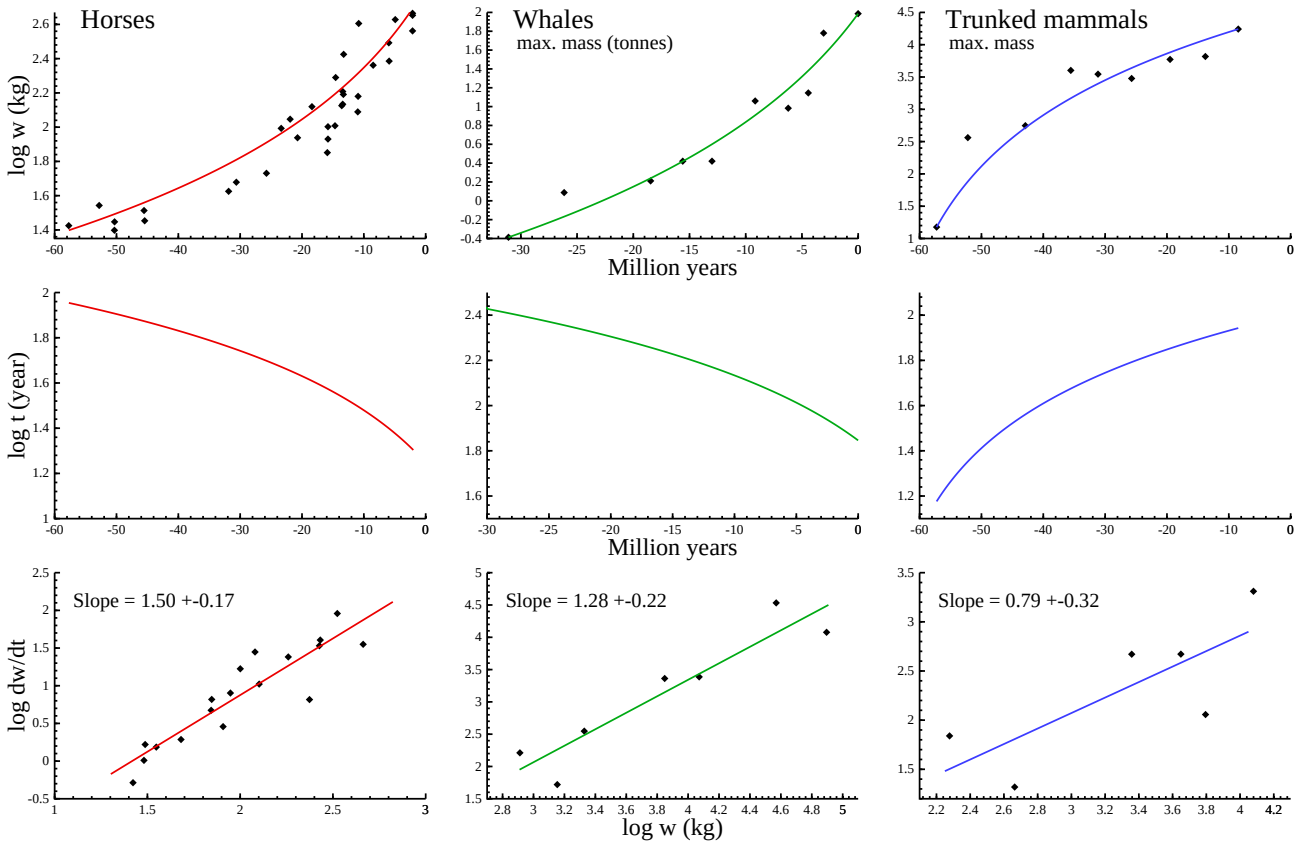

Group	Equidae	Primates	Cetacea Mysticeti	Artiodactyla	Carnivora Fissipedia	Proboscidea	Mammalia
d	2D	3D	3D	2D	2D	2D	2D
dw/dt	1.50 ± 0.17	1.28 ± 0.30	1.28 ± 0.22	1.19 ± 0.24	1.10 ± 0.12	0.79 ± 0.32	0.83 ± 0.20
r_{β_β}/r_α	$\approx \infty$	≈ 1.2	≈ 1.2	≈ 1.4	≈ 0.9	≈ 0.1	≈ 0.1

Figure 4: **Mammalian evolution** of body mass (w; **top**) and lifespan (t; **middle**) in physical time. Trajectories for horses (Equidae; **left**) and for the maximum mass of mammalian clades (**middle, right, table**). The r_{β_β}/r_α-ratio is estimated from the slope of the allometry for the rate of increase in mass (dw/dt, kg per million year) in physical time (**bottom plots**). Fossil horses had an infinite r_{β_β}/r_α-ratio and masses that increased exclusively by evolutionary acceleration (**red**), while most ratios for maximum mass are around one, with a similar increase in metabolism and resource handling (**green**). With a ratio around zero, the increase in maximum mass for trunked mammals (Proboscidea) and all terrestrial mammals is dominated by increased resource handling/availability (**blue**). No taxa showed log-linear evolution along a metabolic bound. Data from MacFadden (1986), Smith et al. (2010) and Okie et al. (2013), Supplementary Tables S1 to S4.

3.1.3 *Maximum mass of terrestrial mammals*

At a next step in ecological scale we have a r_{β_β}/r_α-ratio that approaches zero because improved resource handling and/or resource availability out-runs evolution in process speed. If seen, this evolution should relate to the fastest body mass evolution during pulses of evolutionary radiation. It is not observed in whales, but the $\mathrm{d}w/\mathrm{d}t$ exponent is only slightly larger than the predicted 3/4 for the 2D-evolution of the maximum mass of trunked mammals (Probocidae) over 49 million years, and for the maximum mass of all terrestrial mammals over 100 million years of evolution (Fig. 4).

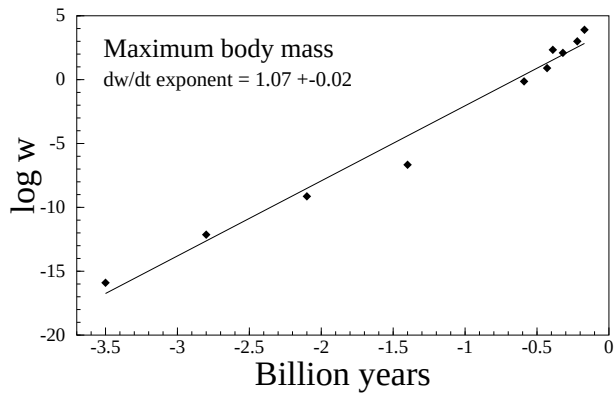

Figure 5: **Macro evolution** The maximum mass (length raised to third power) of mobile organisms over 3.5 billion years of evolution. Data from Bonner (1965), Supplementary Table S5.

3.2 Macro evolution at metabolic limit

With constant selection for increased metabolic pace, macro evolution may reach a biochemical bound on mass specific metabolism. This evolution will follow the yellow curves in Fig. 2 and 3, with a r_{β_β}/r_α-ratio of 1/2 in 2D and 1/4 in 3D. They are log-linear because the upward bend from the time contraction of metabolic acceleration is balanced against the downward bend from the time dilation of mass-rescaling.

The increase in maximum animal mass during the 3.5 billion years of evolution on Earth was not uniform (Payne et al. 2009), but with a $\mathrm{d}w/\mathrm{d}t$ exponent of 1.07 ± 0.02 it is close to log-linear (Witting 2008, Fig. 5, top). This suggest that the macro evolution of major taxonomic groups runs along an upper limit on mass specific metabolism, a conclusion that is supported also by an invariant mass specific metabolism across taxonomic groups from Prokaryotes to mammals (Makarieva et al. 2005, 2008; Kiørboe and Hirst 2014; Witting 2016b).

4 Discussion

4.1 Metabolic time-bend

With mass specific metabolism being selected as the pace of the handling that converts resource energy into replication (Witting 2016a,b), we predict an exponential increase in net energy and mass specific metabolism on the per generation time-scale of the organism. This increase was found in this paper to explain not only a population dynamic feed-back selection for an exponential increase in mass, but also the allometric exponents of a time-bend in body mass trajectories of the fossil record.

Dependent upon the r_{β_β}/r_α-ratio of the exponential increase in pace over handling, the bending exponent ($\hat{d}t$) of the body mass allometry for the rate of change in mass in physical time ($\mathrm{d}w/\mathrm{d}t \propto w^{\hat{d}t}$) was predicted to change from 3/4 to 3/2 given 2D interactions, and from 5/6 to 5/3 given 3D. For unconstrained selection with optimal resource handling in an ecological niche the predicted $\hat{d}t$ exponent is 3/2 in 2D; as observed for mass evolution in horses over the past 57 million years. This corresponds with an infinite r_{β_β}/r_α-ratio and a mass that increases exclusively because of metabolic acceleration.

Unconstrained symmetrical selection across ecological niches correspond with a r_{β_β}/r_α-ratio of one, relating to a body mass evolution where resource handling and pace are equally important for the increase in mass. This may be expected as a base case for the evolution of the maximum mass in taxonomic groups that diversify into a multitude of species across ecological niches. It is associated with $\hat{d}t$ exponents of 9/8 in 2D and 5/4 in 3D, and was found for maximum mass evolution in four out of five mammalian clades.

Other options include fast body mass evolution with a r_{β_β}/r_α-ratio of zero and $\hat{d}t$ exponents of 3/4 in 2D and 5/6 in 3D, in agreement with maximum mass evolution in trunked and all terrestrial mammals. Finally, r_{β_β}/r_α-ratios of $1/2(d-1)$ have log-linear trajectories in physical time ($\hat{d}t = 1$), and they emerge when mass specific metabolism evolves along an upper bound. This appears to be the case for 3.5 billion years of maximum mass evolution across all mobile organisms on Earth.

4.2 Species distributions

These trajectories represent only a fraction of the trajectories in the fossil record. While unlikely unique, the

pure metabolic driven increase of the horse requires conditions where resource handling is optimised for a niche that the evolutionary lineage can maintain and defend in inter-specific competition. And the trajectories of maximum mass evolution represent only the upper boundaries of expanding species distributions. More generally we expect not only time variation, but also lineages that have restricted and variable resource access due to inter-specific interactive competition. This should generate not only evolutionary lineages with variable rates of increase, but also lineages with more stable masses, as well as lineages that decline in mass.

If the inter-specific partitioning of resources over mass follows regular rules we expect, as observed (Trammer 2002, 2005), a rate of radiation that is positively dependent on the maximum mass, with a larger maximum mass allowing for the existence of more species with smaller masses. And as evolutionary lineages are predicted to have an inherent tendency to increase in size, smaller species should increase in size if released from the inter-specific competition of larger species; as observed quite commonly in small lineages on islands with few competing species (Foster 1964; Heaney 1978; Lomolino 1985).

With this study I did not aim for a deduction of the evolutionary unfolding of the life histories for complete species distributions over time. I have though in the supplementary information generated simple simulations for species distributions of multicellular animals over time. These show that evolutionary lineages that diversity with random r_{β_β}/r_α-ratios tend to generate across species allometries with exponents for mass specific metabolism around $-1/2d$. These distributions contain species variation in the pre-mass component of mass specific metabolism, yet, this variation in the mass-rescaling intercept is spread across the distribution of masses with the overall correlation being dominated by variation in the densities and handling of the exploited resources.

The metabolic variation in the simulations was found to produce outlier species, with the typical example being metabolism that increases to a higher than expected value in a small species, and more rarely to a lower than expected value in a large species. This pattern follows from lineages that evolve a small or large body mass at an early stage relative to the other species. They will then evolve over a larger or smaller number of generations that the main clade and, thus, they will have a tendency to evolve a higher or lower metabolic rate. This evolution may explain shrews (*Soricidae*) with strongly increased metabolism (Platt 1974), and bowhead whales (*Balaena mysticetus*) with smaller metabolism than expected from mass alone (George 2009). See also the high metabolism of the honey possum (*Tarsipes rostratus*), and the low metabolism of the southern hairy-nosed wombat (*Lasiorhinus latifrons*), relative to the metabolic allometry for marsupial mammals in Fig. 6.

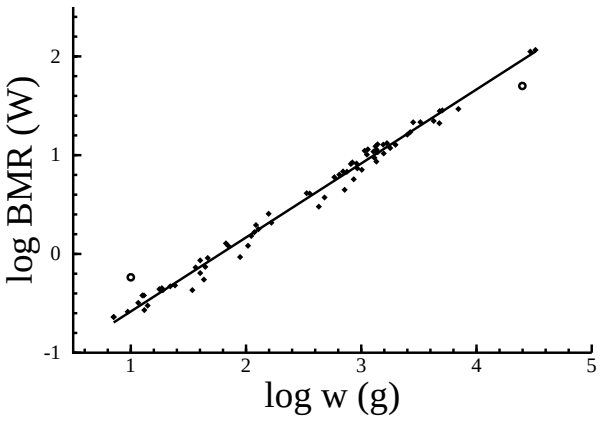

Figure 6: **Marsupial mammals.** The allometric relationship between the basal metabolic rate (BMR) and body mass (w) in marsupial mammals; with an estimated exponent of 0.75 ± 0.01. Data from McNab (2008), with the honey possum (left open circle) and the southern hairy-nosed wombat (right open circle) removed as outliers from the regression.

These outlier species may be part of a more general pattern, where the relationship between metabolism and mass is not a straight allometric line on logarithmic scale, but a bend curve where the smaller species have higher metabolic rates than expected from Kleiber scaling alone (Kolokotrones et al. 2010; MacKay 2011). By using the model that was developed in this paper, I simulate the evolution of the species distributions of placental and marsupial mammals in a separate study (Witting 2016c), and find that the exponential acceleration of metabolism is explaining also the curvature in inter-specific allometric scaling.

The deviations of the outlier species and curvature from typical Kleiber scaling do not reflect adaptations in a traditional sense. Instead they reflect differences in evolutionary time; where each lineage has its own time defined by the number of generations it evolves, with the smallest and largest species tending to evolve through quite a different number of generations than the average species.

4.3 Natural selection time

This natural selection time of the per generation time-scale is an essential feature of biological evolution. It implies that each species has a unique time-scale of natural selection that dilates and contracts relative to physical time with the evolutionary changes in metabolism and mass.

If metabolism is evolving exclusively from mass-rescaling ($r_{\beta_\beta}/r_\alpha = 0$), we have Kleiber scaling for 2D evolution with a natural selection time-scale that dilates to the positive 1/4 power of mass. For 2D evolution at the other extreme, where mass is evolving exclusively from metabolic acceleration ($r_{\beta_\beta}/r_\alpha \approx \infty$), we have a natural selection time that contracts to the negative 1/2 power of mass.

It is this dilation and contraction of the frequency of natural selection changes that bend the log-linear mass trajectory in physical time. And with the actual values of the predicted bends being confirmed by the fossil record, I find that the inclusion of evolutionary changes in natural selection time is essential for the interpretation of evolutionary changes in time.

4.4 The evolutionary arrow of time

With evolutionary trajectories in the fossil record confirming the metabolic time-bend of exponential body mass evolution we have identified an evolutionary arrow of time. By describing the expected when the extrinsic environment is stable, the arrow identifies an overall direction for evolution by natural selection; a direction that is inconceivable with the strong interpretation of the contingent view that states that biotic evolution can only be understood *a posteriori* from its historical development once it has actually occurred (Gould 2002).

It is intriguing that natural selection, which is continent and random at the basic level of genetic mutations, is found to predict the very bend of body mass evolution in time. The hint is population dynamic feed-back selection that is maintained as a dissipative selection by the energy that is allocated into self-replication, population growth and intra-population interactive competition. With a steady influx of energy to the population, this implies a sustained natural selection that chooses an *a priori* determined direction among the randomly generated mutations.

The idea of a direction to evolution by natural selection is not new. Schrödinger (1944), Bertalanffy (1952) and Prigogine (1978) saw biotic systems as dissipative structures that organise themselves through a continued use of the free energy that is available to the open thermodynamic system. This view was developed into a thermodynamic entropy based selection (e.g., Wicken 1985; Brooks and Wiley 1986; Schneider and Kay 1994), and in a somewhat similar way did Lotka (1922), and others (Odum and Pinkerton 1955; Van Valen 1973, 1976; Brown et al. 1993; Brown 1996), see natural selection as a constrained maximisation of the flux of energy through individuals. While biotic evolution is indeed correlated with energy and entropy, these views fail to comply with the most basic Darwinian paradigm; that natural selection operates by differential self-replication, instead of operating directly from energy or other related measures.

Directional evolution by differential self-replication was maybe first proposed by Fisher (1930), when he used frequency independent selection to formulate his fundamental theory of natural selection that predicts a continued increase in the average fitness of the population, measured by either r or n^*. But with r and n^* declining with body mass across species of multicellular animals (Fenchel 1974; Damuth 1981, 1987) it follows that the direction of the fundamental theorem is inconsistent with the existence of large bodied species (see appendix in Witting 2016b).

By using an energetic model to formulate differential self-replication selection by the joint action of the frequency independent selection of the physiology and the density-frequency-dependent selection of interactive competition, I have proposed a theory that explains lifeforms from virus to multicellular animals (Witting 2016b), including major transitions in the life history (Witting 2002) and allometries (Witting 2016a), and the bending of exponential trajectories in physical time (this paper). And with the predicted direction following as an intrinsic property of natural selection, it is expected in a suitable environment with a steady and sufficiently strong influx of energy that can be utilised by biotic organisms.

The predicted evolutionary direction is expected to be reversible, but not strictly symmetrical, if the influx of energy to the overall ecosystem starts to decline at a rate that dominates the selected increase in net energy (Witting 1997, 2008). The overall direction of population dynamic feed-back selection will then be a decline in mass, with the invariance and allometries of mass-rescaling applying also to declining masses (Witting 2016a). While this explains widespread dwarfing during periods of environmental crisis (Guthrie 1984; King and Saunders 1984; Martin and Klein 1984; Barnosky 1989; Donovan 1989; McKinney 1990), the more uncertain response relates to pre-mass selection on metabolic pace. A decline in resource density might stress the energetic

balance ($\epsilon = \epsilon_g - w\beta$) between gross and net resource assimilation, especially in larger species that have to sustain larger metabolic costs ($w\beta$). Such mass dependent distortion might explain the predominant extinction of larger species during mass extinction from environmental crises; but body mass biased extinctions may also reflect a slower evolutionary response in larger species with longer generations.

4.5 Natural selection theory

The theory of evolution by natural selection was created in the shadows of the physical theories. For long it was distinguished by an absence of a general evolutionary direction; a tradition that started when Darwin (1859) proposed that species are best understood from their evolutionary history of common origin.

The absence of a direction driven by universal laws was argued to be something special that distinguished evolutionary biology from the physical sciences (e.g., Mayr 1988; Salthe 1989; Williams 1992; Maynard Smith and Szathmáry 1995; Gould 2002), and it generated the paradigm of contingent evolution by historical natural selection (Witting 2008). Here, evolution – even when caused by natural selection – can only be understood backwards after time's actual unfolding. This thinking is implicit in traditional life history theory (Charlesworth 1980, 1994; Roff 1992, 2002; Stearns 1992), with examples including body mass models that were developed from an evolved correlation between reproduction and mass (Roff 1981; Stearns and Koella 1986), and allometric models that were developed from the very existence of metabolism and mass (West et al. 1997, 1999; Demetrius 2003; Fujiwara 2003; Makarieva et al. 2005; Glazier 2010).

Having developed the alternative hypothesis of directional evolution from the deterministic components of natural selection over the past twenty years, I find that the historical dominance of contingent thinking in natural selection theory arose as a conceptual misunderstanding in a young scientific discipline that had not yet discovered general regularities. In fact, with natural selection emerging from the origin of replicating molecules, I find that evolutionary biology is in the unique position to define a mathematical theory for the natural selection that unfolds deterministically from self-replication. By applying this concept, I have constructed a theory that, even in the absence of parameter estimates from evolved biota, predicts an unfolding that is basically parallel to evolution on Earth. Biological evolution by natural selection is therefore proposed as an inescapable unfolding that follows from the origin of replicating molecules in suitable environments.

References

Barnosky A. D. (1989). The late pleistocene event as a paradigm for wide spreadmammal extinction. In: Donovan S. K. (ed). Mass extinctions. Processes and evidence: Columbia University Press, New York, pp 235–254.

Bertalanffy L. v. (1952). Problems of life. Watts, London.

Bonner J. T. (1965). Size and cycle. Princeton University Press, Princeton.

Broham L. (2011). The genome as a life-history character: why rate of molecular evolution varies between mammal species. Phil. Trans. R. Soc. B: Biol. Sci 366:2503–2513.

Brooks D. R. Wiley E. O. (1986). Evolution as entropy. Cambridge University Press, Cambridge.

Brown J. H. (1996). Macroecology. University of Chicago Press, Chicago.

Brown J. H., Marquet P. A., Taper M. L. (1993). Evolution of body size: Consequences of an energetic definition of fitness. Am. Nat. 142:573–584.

Charlesworth B. (1980). Evolution in age-structured populations. Cambridge University Press, Cambridge.

Charlesworth B. (1994). Evolution in age-structured populations. 2nd edn. Cambridge University Press, Cambridge.

Damuth J. (1981). Population density and body size in mammals. Nature 290:699–700.

Damuth J. (1987). Interspecific allometry of population density in mammals and other animals: the independence of body mass and population energy-use. Biol. J. Linnean Society. 31:193–246.

Darwin C. (1859). The origin of species. John Murray, London.

DeLong J. P., Okie J. G., Moses M. E., Sibly R. M., Brown J. H. (2010). Shifts in metabolic scaling, production, and efficiency across major evolutionary transitions of life. Proc. Nat. Acad. Sci. 107:12941–12945.

Demetrius L. (2003). Quantum statistics and allometric scaling of organisms. Physica 322:477–490.

Donovan, S. K., ed (1989). Mass extinctions: Processes and evidence. Columbia University Press, New York.

Dyson F. W., Eddington A. S., Davidson C. (1920). A determination of the deflection of light by the sun's gravitational field, from observations made at the total eclipse of may 29, 1919. Phil. Trans. R. Soc. Lond. A. 220:291–333.

Fenchel T. (1974). Intrinsic rate of natural increase: The relationship with body size. Oecologia 14:317–326.

Fisher R. A. (1930). The genetical theory of natural selection. Clarendon, Oxford.

Foster J. B. (1964). The evolution of mammals on islands. Nature 202:234–235.

Fujiwara N. (2003). Origin of the scaling rule for fundamental living organisms based on thermodynamics. BioSys. 70:1–7.

Galtier N., Blier P. U., Nabholz B. (2009). Inverse relationship between longevity and evolutionary rate of mitochondrial proteins in mammals and birds. Mitochon. 9:51–57.

George J. C. (2009). Growth, morphology and energetic of bowhead whales (*Balaena mysticetus*). (Thesis, Ph.D.). University of Alaska, Fairbanks.

Gillooly J. F., Allen A. P., West G. B., Brown J. H. (2005). The rate of dna evolution: Effects of body size and temperature on the molecular clock. Proc. Nat. Acad. Sci. USA 102:140–145.

Gingerich P. D. (1993). Quantification and comparison of evolutionary rates. Am. J. Sci. 293A:453–478.

Glazier D. S. (2010). A unifying explanation for diverse metabolic scaling in animals and plants. Biol. Rev. 85:111–138.

Gould S. J. (2002). The structure of evolutionary theory. The Belknap Press of Harvard University Press, Cambridge.

Guthrie R. D. (1984). Mosaic, allelochemics and nutrients. an ecological theory of late pleistocene megafaunal extinctions. In: Martin P. S. Klein R. G. (eds). Quaternary extinctions. A prehistoric revolution: The University of Arizona Press, Tucson, pp 259–298.

Hayami I. (1978). Notes on the rates and patterns of size change in evolution. Paleobiology 4:252–260.

Heaney L. R. (1978). Island area and body size of insular mammals: evidence from the tri-colored squirrel (*callosciurus prevosti*) of southeast asia. Evolution 32:29–34.

King J. E. Saunders J. J. (1984). Environmental insularity and the extinction of the american mastodont. In: Martin P. S. Klein R. G. (eds). Quaternary extinctions. A prehistoric revolution: The University of Arizona Press, Tucson, pp 315–344.

Kiørboe T. Hirst A. G. (2014). Shifts in mass scaling of respiration, feeding, and growth rates across life-form transitions in marine pelagic organisms. Am. Nat. 183:E118–E130.

Kleiber M. (1932). Body and size and metabolism. Hilgardia 6:315–353.

Kolokotrones T., Savage V., Deeds E. J., Fontana W. (2010). Curvature in metabolic scaling. Nature 464:753–756.

Lomolino M. (1985). Body size of mammals on islands: the island rule reexamined. Am. Nat. 125:310–316.

Lotka A. J. (1922). Contribution to the energetics of evolution. Proc. Nat. Acad. Sci. 8:147–151.

Lynch M. (1990). The rate of morphological evolution in mammals from the standpoint of the neutral expectation. Am. Nat. 136:727–741.

MacFadden B. J. (1986). Fossil horses from "eohippus" (hyracotherium) to equus: scaling, cope's law, and the evolution of body size. Paleobiology 12:355–369.

MacKay N. J. (2011). Mass scale and curvature in metabolic scaling. J. theor. Biol. 280:194–196.

Makarieva A. M., Gorshkov V. G., Bai-Lian L. (2005). Energetics of the smallest: do bacteria breathe at the same rate as whales. Proc. R. Soc. B. 272:2219–2224.

Makarieva A. M., Gorshkov V. G., Li B., Chown S. L., Reich P. B., Gavrilov V. M. (2008). Mean mass-specific metabolic rates are strikingly similar across life's major domains: Evidence for life's metabolic optimum. Proc. Nat. Acad. Sci. 105:16994–16999.

Martin A. P. Palumbi S. R. (1993). Body size, metabolic-rate, generation time, and the molecular clock. Proc. Nat. Acad. Sci. USA 90:4078–4091.

Martin, P. S. & Klein, R. G., eds (1984). Quaternary extinctions. A prehistoric revolution. The University of Arizona Press, Tucson.

Maynard Smith J. Szathmáry E. (1995). The major transitions in evolution. W.H. Freeman Spektrum, Oxford.

Mayr E. (1988). Toward a new philosophy of biology. Observations of an evolutionist. Harvard University Press, Cambridge.

McKinney M. L. (1990). Trends in body-size evolution. In: McNamara K. J. (ed). Evolutionary Trends: The University of Arizona Press, Tucson, pp 75–118.

McNab B. K. (2008). An analysis of the factors that influence the level and scaling of mammalian bmr. Comp. Bioch. Physiol. A 151:5–28.

Nabholz B., Glemin S., Galtier N. (2008). Strong variations of mitochondrial mutation rate across mammals the longevity hypothesis. Mol. Biol. Evol. 25:120–130.

Newton I. (1687). Philosophiæ Naturalis Principia Mathematica. London.

Odum H. T. Pinkerton R. C. (1955). Times speed regulator the optimum efficiency for maximum power output in physical and biological systems. Am. Sci. 43:331–343.

Okie J. G., Boyer A. G., Brown J. H., Costa D. P., Ernest S. K. M., Evans A. R., Fortelius M., Gittleman J. L., Hamilton M. J., Harding L. E., Lintulaakso K., Lyons S. K., Saarinen J. J., Smith F. A., Stephens P. R., Theodor J., Uhen M. D., Sibly R. M. (2013). Effects of allometry, productivity and lifestyle on rates and limits of body size evolution. Proc. R. Soc. B. 280:20131007.

O'Leary M., Bloch J. I., Flynn J. J., Gaudin T. J., Gillombardo A., Giannini N. P., Goldberg S. L., Kraatz B. P., Luo Z., Meng J., Ni X., Novacek M. J., Perini F. A., Randall I. Z. S., Rougier G. W., Sargis E. J., Silcox M. T., Simmons N. B., Spaulding M., Velazco P. M., Weksler M., Wible J. R., Cirranello A. L. (2013). The placental mammal ancestor and the post-k-pg radiation of placentals. Science 339:662–667.

Payne J. L., Boyer A. G., Brown J. H., Finnegan S.,

Kowalewski M., Krause R. A., Lyons J. S. K., McClain C. R., McShea D. W., Novack-Gottshall P. M., Smith F. A., Stempien J. A., Wang S. C. (2009). Two-phase increase in the maximum size of life over 3.5 billion years reflect biological innovation and environmental opportunity. Proc. Nat. Acad. Sci. 106:24–27.

Peters R. H. (1983). The ecological implication of body size. Cambridge University Press, Cambridge.

Platt W. J. (1974). Metabolic rates of short-tailed shrews. Physiol. Zool. 42:75–90.

Prigogine I. (1978). Time, structure, and fluctuations. Science 201:777–785.

Robertson A. (1968). The spectrum of genetic variation. In: Lewontin R. C. (ed). Population Biology and Evolution: Syracuse University Press, New York, pp 5–16.

Roff D. A. (1981). On being the right size. Am. Nat. 118:405–422.

Roff D. A. (1992). The evolution of life histories. Theory and analysis. University of Chicago Press, New York.

Roff D. A. (2002). Life history evolution. Sinauer Associates, Inc., Massachusetts.

Salthe S. N. (1989). Untitled. In: Hecht M. K. (ed). Evolutionary biology at the crossroads: Queens College Press, New York, pp 174–176.

Scheider E. D. Kay J. J. (1994). Life as a manifestation of the second law of thermodynamics. Math. Comput. Model. 19:25–48.

Schrödinger E. (1944). What is life? Cambridge University Press, Cambridge.

Smith F. A., Boyer A. G., Brown J. H., Costa D. P., Dayan T., Ernest S. K. M., Evans A. R., Fortelius M., Gittleman J. L., Hamilton M. J., Harding L. E., Lintulaakso K., Lyons S. K., McCain C., Okie J. G., Saarinen J. J., Sibly R. M., Stephens P. R., Theodor J., Uhen M. D. (2010). The evolution of maximum body size of terrestrial mammals. Science 330:1216–1219.

Stearns S. C. (1992). The evolution of life histories. Oxford University Press, Oxford.

Stearns S. C. Koella J. (1986). The evolution of phenotypic plasticity in life-history traits: Predictions for norms of reaction for age- and size-at-maturity. Evolution 40:893–913.

Taylor P. D. (1996). The selection differential in quantitative genetics and ess models. Evolution 50:2106–2110.

Trammer J. (2002). Power formula for copes rule. Evol. Ecol. Res. 4:147–153.

Trammer J. (2005). Maximum body size in a radiating clade as a function of time. Evolution 59:941–947.

Van Valen L. (1973). A new evolutionary law. Evol. Theory 1:1–30.

Van Valen L. (1976). Energy and evolution. Evol. Theory 1:179–229.

West G. B., Brown J. H., Enquist B. J. (1997). A general model for the origin of allometric scaling laws in biology. Science 276:122–126.

West G. B., Brown J. H., Enquist B. J. (1999). The fourth dimension of life: fractal geometry and allometric scaling of organisms. Science 284:1677–1679.

Wicken J. S. (1985). Thermodynamics and the conceptual structure of evolutionary theory. J. theor. Biol. 117:363–383.

Williams G. C. (1992). Natural selection. Domains, levels, and challenges. Oxford University Press, New York.

Witting L. (1995). The body mass allometries as evolutionarily determined by the foraging of mobile organisms. J. theor. Biol. 177:129–137.

Witting L. (1997). A general theory of evolution. By means of selection by density dependent competitive interactions. Peregrine Publisher, Århus, 330 pp, URL http://mrLife.org.

Witting L. (2002). From asexual to eusocial reproduction by multilevel selection by density dependent competitive interactions. Theor. Pop. Biol. 61:171–195.

Witting L. (2003). Major life-history transitions by deterministic directional natural selection. J. theor. Biol. 225:389–406.

Witting L. (2008). Inevitable evolution: back to *The Origin* and beyond the 20th Century paradigm of contingent evolution by historical natural selection. Biol. Rev. 83:259–294.

Witting L. (2016a). The natural selection of metabolism and mass selects allometric transitions from prokaryotes to mammals. bioRxiv http://dx.doi.org/10.1101/084624.

Witting L. (2016b). The natural selection of metabolism and mass selects lifeforms from viruses to multicellular animals. bioRxiv http://dx.doi.org/10.1101/087650.

Witting L. (2016c). The natural selection of metabolism explains curvature in allometric scaling. bioRxiv Coming soon.

Supplementary Tables

Nr	Species pair	w_0	w_1	$\bar{w}$	Δt	dw/dt
1	Hyracotherium angustidens - Hyracotherium tapirinum	26.6	34.9	30.8	5.0	1.7
2	Hyracotherium angustidens - Hyracotherium vaccassiense	26.6	24.9	25.8	5.0	-0.3
3	Hyracotherium vaccassiense - Orohippus pumulis	24.9	28.0	26.5	6.0	0.5
4	Orohippus pumulis - Epihippus gracilis	28.0	28.4	28.2	4.0	0.1
5	Orohippus pumulis - Epihippus uintensis	28.0	32.6	30.3	4.5	1.0
6	Epihippus gracilis - Mesohippus bairdii	28.4	42.2	35.3	9.0	1.5
7	Mesohippus bairdii - Miohippus quartus	42.2	53.8	48.0	6.0	1.9
8	Miohippus quartus - Parahippus tyleri	53.8	86.7	70.3	5.0	6.6
9	Miohippus quartus - Archaeohippus blackbergi	53.8	43.9	48.9	7.0	-.4
10	Parahippus tyleri - Parahippus leonesis	86.7	76.6	81.7	2.0	-5.1
11	Parahippus leonesis - Merychippus isonesus	76.6	85.2	80.9	3.0	2.9
12	Parahippus leonesis - Merychippus insignis	76.6	100.6	88.6	3.0	8.0
13	Anchitherium clarenci - Hypohippus sp.	131.7	403.0	267.4	8.0	33.9
14	Merychippus insignis - Hipparion shirleyi	100.6	77.5	89.1	2.0	-1.6
15	Hipparion shirleyi - Hipparion tehonense	77.5	122.8	100.2	2.7	16.8
16	Cormohipparion goorisi - Cormohipparion occidentale	101.9	151.3	126.6	4.7	10.5
17	Merychippus insignis - Nannippus minor	100.6	59.6	80.1	7.0	-5.9
18	Merychippus isonesus - Pliohippus pernix	85.2	155.3	120.3	2.5	28.0
19	Dinohippus sp. - Dinihippus leidyanus	133.5	229.9	181.7	4.0	24.1
20	Dinihippus leidyanus - Dinihippus galushai	229.9	310.7	270.3	2.0	40.4
21	Dinihippus leidyanus - Dinihippus mexicanus	229.9	243.0	236.5	2.0	6.6
22	Dinihippus mexicanus - Equus simplicidens	243.0	424.7	333.9	2.0	90.9
23	Nannippus minor - Nannippus peninsulatus	59.6	79.9	69.8	4.3	4.7
24	Equus simplicidens - Equus scotti	424.7	495.6	460.2	2.0	34.5

Table S1: Rates of body mass evolution for 24 plausible ancestral-descendant species pairs of North American fossil horses. Only positive rates of evolution were used for the estimate of the dt/dt exponent, with one outlier removed (pair nr 4). w in kg, t in million years, dw/dt in kg/million year. Data from MacFadden (1986).

Group	w	t	Δw	Δt	$\bar{w}$	dw/dt
Artiodactyla	7255	49.5	2141	1.8	6184.5	1215.1
Artiodactyla	5114	47.7	2952	4	3638	737.1
Artiodactyla	2162	43.7	-	-	-	-
Artiodactyla	3005	38.4	1486	5.7	2262	260.2
Artiodactyla	1519	32.7	-	-	-	-
Artiodactyla	1519	26.5	-	-	-	-
Artiodactyla	1829	21.1	1332	4.4	1163	302.7
Artiodactyla	497	16.7	132	7.4	431	18
Artiodactyla	365	9.3	330	9.3	200	35.5
Artiodactyla	35	0	-	-	-	-
Carnivora/Fissipedia	3692	63.6	-	-	-	-
Carnivora/Fissipedia	3692	63.6	1992	0.9	2696	2217
Carnivora/Fissipedia	1700	62.7	924	1.8	1238	513.5
Carnivora/Fissipedia	776	60.9	-	-	-	-
Carnivora/Fissipedia	1700	59.1	-	-	-	-
Carnivora/Fissipedia	4665	55.1	4265	5.3	2532.5	801.7
Carnivora/Fissipedia	400	49.8	-	-	-	-
Carnivora/Fissipedia	689.3	44.1	358.3	6.2	510.2	57.7
Carnivora/Fissipedia	331	37.9	109.4	5.4	276.3	20.1
Carnivora/Fissipedia	221.6	32.5	216.7	4.4	113.3	49.2
Carnivora/Fissipedia	4.9	28.1	3.4	7.4	3.3	0.5
Carnivora/Fissipedia	1.6	20.7	-	-	-	-
Carnivora/Fissipedia	5.3	11.4	-	-	-	-
Carnivora/Fissipedia	5.3	6.4	-	-	-	-
Carnivora/Fissipedia	10	3.4	7.4	3.4	6.3	2.2
Carnivora/Fissipedia	2.6	0	-	-	-	-
Primates	500	54.5	404	1.8	298	229.3
Primates	96	52.8	-	-	-	-
Primates	225	48.8	175	5.3	137.5	32.9
Primates	50	43.5	-	-	-	-
Primates	50	37.8	47.3	6.2	26.4	7.6
Primates	2.7	31.5	-	-	-	-
Primates	7.9	26.1	-	-	-	-
Primates	8.6	21.7	-	-	-	-
Primates	9	14.4	2.7	9.3	7.7	0.3
Primates	6.3	5.1	6.2	5.1	3.2	1.2
Primates	0.1	0	-	-	-	-
Proboscidea	17450	48.8	10882	5.3	12009	2045.5
Proboscidea	6568	43.5	651	5.7	6242.5	114
Proboscidea	5917	37.8	2917	6.2	4458.5	469.3
Proboscidea	3000	31.5	-	-	-	-
Proboscidea	3500	26.1	-	-	-	-
Proboscidea	4000	21.7	3442	7.4	2279	468.3
Proboscidea	558	14.4	194	9.3	461	20.9
Proboscidea	364	5.1	349	5.1	189.5	69.1
Proboscidea	15	0	-	-	-	-

Table S2: Maximum body mass, and rates of maximum body mass evolution, for mammalian clades. Only positive rates shown and used. t in millions of years ago, w in kg. Data from Okie et al. (2013).

Group	w	t	Δw	Δt	$\bar{w}$	dw/dt
Cetacea/Mysticeti	190000	31.1	93023.6	0	-	-
Cetacea/Mysticeti	96976.4	31.1	36677.1	3.1	78637.8	11946.9
Cetacea/Mysticeti	60299.3	28.1	46331.9	1.4	37133.3	34067.5
Cetacea/Mysticeti	13967.4	26.7	4350.2	1.8	11792.3	2437.1
Cetacea/Mysticeti	9617.2	24.9	-	-	-	-
Cetacea/Mysticeti	11476.3	22	8842.3	3.8	7055.1	2302.7
Cetacea/Mysticeti	2634	18.2	-	-	-	-
Cetacea/Mysticeti	2634	15.6	1007.6	2.9	2130.2	352.3
Cetacea/Mysticeti	1626.3	12.7	403.3	7.7	1424.7	52.4
Cetacea/Mysticeti	1223.1	5	813	5	816.6	162.6
Cetacea/Mysticeti	410.1	0	-	-	-	-

Table S3: Maximum body mass, and rates of maximum body mass evolution, for Cetacea/Mysticeti. Only positive rates shown and used, and one outlier removed. t in million of years ago, w in kg. Data from Okie et al. (2013).

w	t	Δw	Δt	dw/dt
10000	105.5	-	-	-
15000	104.6	-	-	-
17450	102.8	-	-	-
17450	101	-	-	-
17450	97.0	10882	5.32	2045
6568	91.7	651	5.71	114
5917	86.0	-	-	-
15000	79.8	-	-	-
15000	74.4	9093	4.40	2067
5907	70.0	1407	7.35	191
4500	62.6	3800	9.30	408
700	53.3	-	-	-
700	48.3	646	2.95	219
54	45.3	-	-	-
54	41.9	50.7	7	7.2
3.3	34.9	-	-	-
5	0	-	-	-

Table S4: Maximum body mass, and rates of maximum body mass evolution, for all terrestrial mammals. Only positive rates shown and used. t in million of years ago, w in kg. Data from Smith et al. (2010).

t	$\log w$	$\log dw/dt$
-3.5	-5.9	-
-2.8	-2.1	-2.0
-2.1	-9.1	-9.0
-.4	-6.7	-6.5
-0.6	-0.1	0.05
-0.4	0.9	1.7
-0.4	2.3	3.7
-0.3	2.1	-
-0.2	3.0	3.9
-0.2	3.9	5.1

Table S5: Maximum body mass, and rates of maximum body mass evolution, over 3.5 billion years of evolution. Only positive rates shown and used. t in billions of years ago, w in proxy estimated as length raised to the third power. Data from Bonner (1965).

References

Bonner J. T. (1965). Size and cycle. Princeton University Press, Princeton.

MacFadden B. J. (1986). Fossil horses from "eohippus" (hyracotherium) to equus: scaling, cope's law, and the evolution of body size. Paleobiology 12:355–369.

Okie J. G., Boyer A. G., Brown J. H., Costa D. P., Ernest S. K. M., Evans A. R., Fortelius M., Gittleman J. L., Hamilton M. J., Harding L. E., Lintulaakso K., Lyons S. K., Saarinen J. J., Smith F. A., Stephens P. R., Theodor J., Uhen M. D., Sibly R. M. (2013). Effects of allometry, productivity and lifestyle on rates and limits of body size evolution. Proc. R. Soc. B. 280:20131007.

Smith F. A., Boyer A. G., Brown J. H., Costa D. P., Dayan T., Ernest S. K. M., Evans A. R., Fortelius M., Gittleman J. L., Hamilton M. J., Harding L. E., Lintulaakso K., Lyons S. K., McCain C., Okie J. G., Saarinen J. J., Sibly R. M., Stephens P. R., Theodor J., Uhen M. D. (2010). The evolution of maximum body size of terrestrial mammals. Science 330:1216–1219.

Supplementary Information

In this section I simulated the evolution of species distributions to examine when we can expect mass-rescaling allometries (1/4 and 1/6 exponents for lifespan) across species that have evolved over time with different r_{β_β}/r_α-ratios.

Species distributions were simulated from a 125 gram ancestor that lived 65 MA by an initial differentiation into 15 evolutionary lineages that evolved at evolutionary steady states during an initial period (T_0) from 65 MA to 30 MA, where each lineage diversified into 15 species, with species evolving at evolutionary steady states during a second period (T_1) until 0 MA. Lineages and species were assigned evolutionary rates at random from uniform distributions [$\sim U(\min, \max)$], and species distributions were truncated at 2 grams and 20 tonnes by excluding lineages and species that evolved beyond these limits.

To parametrize the different evolutionary steady states I assumed an initial generation time of 30 years and assigned values to r_ϵ and r_{β_β}. From this I estimated $r_\alpha = r_\epsilon - r_{\beta_\beta}$ as the joint exponential change in $\dot{\alpha}$ and ρ with $\alpha = \dot{\alpha}\rho$, allowing for an exponential decline due to changing environmental (ρ) conditions. With r_h being the estimated r_ϵ for fossil horses, for each lineage I drew r_ϵ from $\sim U(-10r_h, +10r_h)$ for T_0, and then resampled r_ϵ from $\sim U(-15r_h, +15r_h)$ for each species for T_1. Relating to the rate of evolution in the pre mass component of mass specific metabolism I drew r_{β_β} rates from $\sim U(r_{\beta_{\beta,a}} r_h, r_{\beta_{\beta,b}} r_h)$ for T_0, with $r_{\beta_{\beta,a}}$ being a minimum, and $r_{\beta_{\beta,b}}$ a maximum value.

I constructed three different models to assign r_{β_β} rates to the species in T_1. A stop model (S) sat $r_{\beta_\beta} = 0$ for all species in T_1. A resample model (R) resampled r_{β_β} from $\sim U(r_{\beta_{\beta,a}} r_h, r_{\beta_{\beta,b}} r_h)$ for all species in T_1. And a maintained model (M) maintained the lineage specific r_{β_β} from T_0 to all the species of a lineage in T_1. An example of a simulated body mass distribution is shown in Fig. 1, together with the resulting lifespan allometry.

For each model I simulated 1000 species distributions to estimate an average lifespan exponents ($\hat{\tau}$) with an associated standard error, and this was done for different values of $r_{\beta_{\beta,a}}$ and $r_{\beta_{\beta,b}}$, with results shown in Fig. 1.

The results show that mass-rescaling exponents can

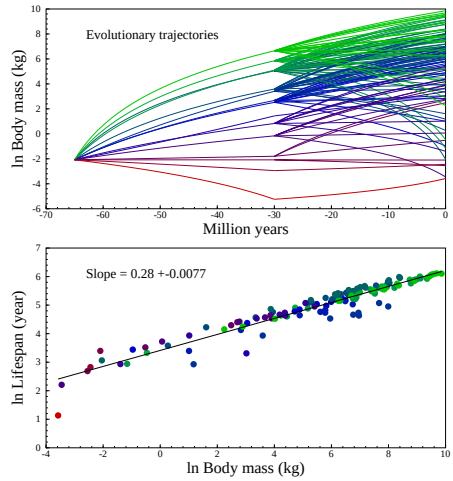

$r_{\beta_{\beta,a}}$	$r_{\beta_{\beta,b}}$	S	R	M
0.0	0.0	0.25	0.25	0.25
1.0	1.0	0.25	0.34	0.34
0.0	1.0	0.24	0.27	0.25
0.0	2.0	0.24	0.27	0.24
0.5	1.5	0.25	0.31	0.29
-1.0	1.0	0.19	0.18	0.15
-2.0	2.0	0.15	0.14	0.11

Figure 1: **2D lifespan exponents** estimated from simulated species distributions. Distributions were truncated at 2 gram and 20 tonnes, and they evolved from random parameterisation of steady state selection in two periods (T_0 & T_1), with 15 lineages evolving from 65 to 30 MA, and each lineage splitting into 15 species at 30 MA, with species evolution to 0 MA. The top plot shows time trajectories and the bottom plot the resulting allometry. Note, that the smallest species was small for the whole period. It evolved through more generations than the other species, and thus it evolved a shorter lifespan, and a higher metabolic rate, than expected when corrected only for size. The table shows average exponents for 1000 species distributions across different models (SE= 0.00 for all models): $r_\epsilon \sim U(-0r_h, +10r_h)$ for T_0, resampled from $\sim U(-5r_h, +15r_h)$ for T_1, with r_h being the r_ϵ estimate for fossil horses. $r_{\beta_\beta} \sim U(r_{\beta_{\beta,a}} r_h, r_{\beta_{\beta,b}} r_h)$ for T_0. Model S: $r_{\beta_\beta} = 0$ for T_1. Model R: r_{β_β} resampled from $\sim U(r_{\beta_{\beta,a}} r_h, r_{\beta_{\beta,b}} r_h)$ for T_1. Model M: r_{β_β} maintained from T_0 to T_1.

be expected as approximations for a wide variety of species distributions. When the metabolic rate behaves as expected, i.e., with an exponential increase over time ($r_{\beta_{\beta,a}} \geq 0$), a close approximation is more often the rule than the exception. If the metabolic rate behaves unexpected instead, i.e., with a decline in a large fraction of species ($r_{\beta_{\beta,a}} < 0$), we may observe deviations from the expected exponents.